International Journal of Petroleum and Gas Exploration Management
Vol.5, No.1, pp.1-14, March 2021
Published by ECRTD-UK
Print ISSN: (Print) ISSN 2515-0863
Online ISSN: (Online) ISSN 2515-0871

ROCK MECHANICS EFFECT ON FRACTURE GEOMETRY AND DIMENSIONLESS FRACTURE CONDUCTIVITY OF 2D MODEL KGD (KHRISTIANOVIC-GEERTSMA-DE KLERK) IN AIR BENAKAT FORMATION, MERUAP FIELD

M. D. Suryadinata[1], D. R. Ratnaningsih[1], I. K. Ariadi[2], F. Waliy[1]*, W. A. Nugroho[1]

[1]Petroleum Engineering Department, Faculty of Mineral Technology, Universitas Pembangunan Nasional Veteran Yogyakarta
[2]Reservoir Engineer, Samudra Energy BWP Meruap
*Email: faizal.waliy.97@gmail.com

ABSTRACT: *Hydraulic fracturing plays a great role in enhancing oil and gas reserves and daily production, and it has been, and will remain, one of the primary engineering tools for improving well productivity. This paper will discuss the effect of rock mechanics (Young's modulus and Poisson's ratio) on fracture geometry (fracture length and width) and dimensionless fracture conductivity designed using 2D model of KGD (Khristianovic-Geertsma-de Klerk), one of the hydraulic fracturing method proposed by Khristianovic & Zheltov (1955) and improved by Geertsma & de Klerk (1969). The study is carried out by doing sensitivity analysis on rock mechanics to the fracture geometry and dimensionless fracture conductivity calculation. The base result of fracture geometry created are respectively 57.552 ft and 0.231 inches of fracture length and width, with reservoir pay zone of 143 ft and dimensionless fracture conductivity of 4.449, after doing 16 iterations of calculation, the results are obtained with a final error percentage of 7.4×10^{-10} %. As the sensitivity analysis is done, results present the same effect between Young's modulus and Poisson's ratio on the fracture geometry and dimensionless fracture conductivity. The higher Young's modulus or Poisson's ratio obtained, the fracture length goes longer, the fracture width goes tiner, while dimensionless fracture conductivity goes lower. Otherwise, the lower Young's modulus or Poisson's ratio obtained, the fracture length goes shorter, the fracture width goes wider, while dimensionless fracture conductivity goes higher. Integrated approaches of empirical relationship are also generated to estimate easily the dimensionless fracture conductivity and fracture geometry of length and width with a certain value of Young's modulus and Poisson's ratio.*

KEYWORDS: KGD, Fracture Geometry, Dimensionless Fracture Conductivity, Rock Mechanics, Young's Modulus, Poisson's Ratio.

INTRODUCTION

Gidley, et al. (1989) showed portrays a conceptual version of the "typical" fracturing process. They said, it consists of blending special chemicals to make the appropriate fracturing fluid and then pumping the blended fluid into the pay zone at high enough rates and pressures to wedge and extend a fracture hydraulically. First, a neat fluid,

called a "pad," is pumped to initiate the fracture and to establish propagation. This is followed by a slurry of fluid mixed with a propping agent (often called a "proppant"). This slurry continues to extend the fracture, and concurrently carries the proppant deeply into the fracture. After the materials are pumped, the fluid chemically breaks back to a lower viscosity and flows back out of the well, leaving a highly conductive propped fracture for oil and/or gas to flow easily from the extremities of the formation into the well (Gidley, et al., 1989).

Hydraulic fracturing plays a great role in enhancing oil and gas reserves and daily production. Hydraulic fracturing has been, and will remain, one of the primary engineering tools for improving well productivity. This is achieved by placing a conductive channel through near-wellbore damage, bypassing this crucial zone; extending the channel to a significant depth into the reservoir to further increase productivity; and placing the channel such that fluid flow in the reservoir is altered (Economides & Nolte, 2000). This paper will discuss one of the hydraulic fracturing methods, that is 2D model of KGD (Khristianovic-Geertsma-de Klerk) promoted by Khristianovic & Zheltov (1955) and improved by Geertsma & de Klerk (1969).

The objective of this paper is to understand the effects of rock mechanics on fracture geometry and dimensionless fracture conductivity designed using the 2D model of KGD. The focused study of rock mechanics are Young's modulus and Poisson's ratio, while the focused fracture geometry are fracture length and width. The study is carried out by doing sensitivity analysis on Young's modulus and Poisson's ratio to the fracture geometry (fracture length and width) and dimensionless fracture conductivity.

ROCK MECHANICS

P-Wave and S-Wave Velocities

Castagna et al. (1985) generated the compressional ratio to shear wave velocity (Waliy et al., 2020b). The Vp/Vs relationship famous established for mudrock line, water-saturated siliciclastic rocks composed primarily of quartz and clay minerals (Castagna et al., 1985). The Vp/Vs relationship is:

$$Vs = 0.862\ Vp - 1.172 \quad (1)$$

where the P-wave and S-wave velocities are in km/s. Later, Castagna et al. (1993) proposed the equation for clastic rock reads:

$$Vs = 0.804\ Vp - 0.856 \quad (2)$$

Dvorkin (2007) proposed the equations according to porosity ranges, as it parted for porosity below 0.15 and exceeding 0.15 respectively:

$$Vs = 0.853\ Vp - 1.137 \quad (3)$$

$$Vs = 0.756\ Vp - 0.662 \quad (4)$$

Young's Modulus

The Young's modulus was computed from the line resulting from the average of the load-deformation curves obtained during a second test (uniaxial compression test) by the usual stress-strain formula (Heindl & Mong, 1936). Static Young's modulus based on uniaxial compression test (UCS) can be estimated:

$$E = \frac{stress}{-strain} = \frac{\sigma}{\varepsilon} \quad (5)$$

Dynamic Young's modulus of rock can be determined using empirical equations obtained from the P-wave velocity and S-wave velocity data (Buntoro, et al., 2018). Fjær et al. (2008) generated an empirical relationship of Poisson's ratio from well log data, sonic and density log, as shown below:

$$E = \rho \times \mathrm{Vs}^2 \frac{(3V_p{}^2 - 4V_s{}^2)}{(V_p{}^2 - V_s{}^2)} \quad (6)$$

where E is Young's modulus in GPa and ρ in gr/cc.

Poisson's Ratio

If a solid body is subjected to an axial tension, it contracts laterally, on the other hand, if it is compressed, the material expands sidewise. So the definition of Poisson's ratio can be stated as the ratio of transverse strain to axial strain induced by unconfined axial deformation (Kumar, 1976). Static Poisson's ratio based on the uniaxial compression test (UCS) can be estimated:

$$v = \frac{lateral\ strain}{axial\ strain} = \frac{\varepsilon_x}{\varepsilon_z} \quad (7)$$

Dynamic Poisson's rock ratio can be determined using empirical equations obtained from the P-wave velocity and S-wave velocity data (Buntoro, et al., 2018). Zoback (2007) generated an empirical equation of Poisson's ratio from well log data of the sonic log, as shown below:

$$v = \frac{V_p{}^2 - 2V_s{}^2}{2(V_p{}^2 - V_s{}^2)} \quad (8)$$

THE KGD (Khristianovic-Geertsma-de Klerk) MODEL

The vertical fracture was first studied by Khristianovic & Zheltov (1955). They stated the fractures are formed in the plane, perpendicular to that of the formation "vertical cracks", in case of hydraulic rupture of the formation by highly viscous, hard penetrating or non-penetrating liquid (Khristianovic & Zheltov, 1955). Geertsma & de Klerk (1969) developed the approach was made obsolete by Khristianovic & Zheltov (1955), generally known as the KGD. An important forerunner to the KGD study is the work by Khristianovic & Zheltov (1955), who introduced the concept of mobile equilibrium-i.e., slow-moving fracture propagation as a result of hydraulic action (Economides & Nolte, 2000).

Khristianovic & Zheltov (1955) assumed plane strain in the horizontal direction, all horizontal cross-sections act independently or equivalently, and all sections are identical (Fig. 1), which is equivalent to assuming that the fracture width changes much more slowly vertically along the fracture face from any point on the face than it does horizontally (Economides & Nolte, 2000). This assumption is correct if the fracture height is much greater than the length. However, applied in practice over full productive intervals, the model yields relatively large fracture widths that seem to be closer to reality in many field cases than the narrower fractures predicted by the PKN theory (Gidley, et al., 1989).

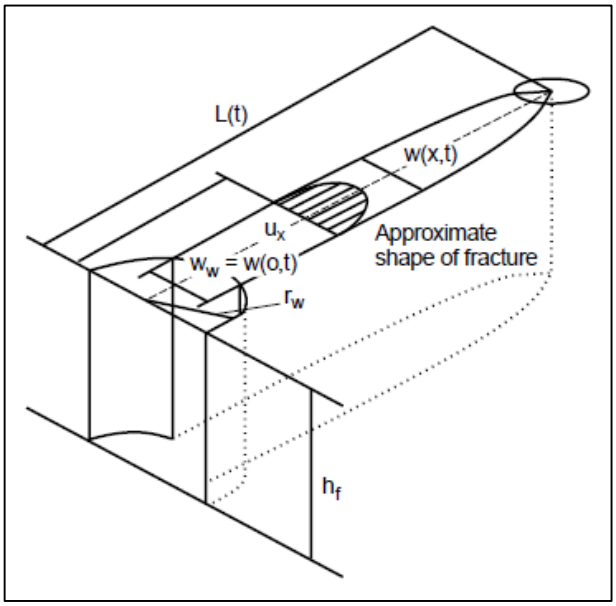

Figure 1. Schematic representation of linearly propagating fracture with the laminar fluid flow according to the KGD model (Gidley, et al., 1989, modified by Economides & Nolte, 2000)

Geertsma & de Klerk (1969) explained the assumptions in the KGD model for vertical linear fracture propagation, as follows: 1) the formation is homogeneous and isotropic as regards those of its properties that influence the fracture-propagation process; 2) the deformations of the formation during fracture propagation can be derived from linear elastic stress-strain relations; 3) the fracturing fluid behaves like a purely viscous liquid; i.e., any peculiar flow behavior due to the addition of gelling agents or other additives is neglected. Moreover, the effect of the propping agent distribution on the distribution of fluid viscosity in the fracture is not taken into account.; 4) Fluid flow in the fracture is everywhere laminar; 5) Simple geometric fracture-extension patterns are assumed - either radially symmetrical propagation from a point source or rectilinear propagation originating from a line source; 6) a rectilinear propagation mode can be accomplished only by injection over a large perforated interval, thus forming a lime source.

Economides and Nolte (2000) explained the fracture geometry and dimensionless fracture conductivity calculations sequentially from the plane strain modulus, maximum fracture width, average fracture width, turbulent flow correction factor, fracture length, and dimensionless fracture geometry. The plane strain modulus can be calculated:

$$E' = \frac{E}{(1-\nu^2)} \qquad (9)$$

where E' is plane strain modulus in Pa, E is Young's modulus in Pa, and ν is Poisson's ratio. Yang (2012) comprehensively explained the equation for estimating the maximum fracture width, as shown below:

$$w_0 = 11.1^{\frac{1}{(2n'+2)}} \times 3.24^{\frac{n'}{(2n'+2)}} \times \left[\frac{1+2n'}{n'}\right]^{\frac{n'}{(2n'+2)}} \times K'^{\frac{1}{(2n'+2)}} \times \left[\frac{q_i^{n'} \times X_f^2}{h_f^{(1-n')} \times E'}\right]^{\frac{1}{(2n'+2)}} \qquad (10)$$

where w_0 is maximum fracture width in inch, n' is power-law effective index typically from 0 to 1 (Economides & Nolte, 2000), K' is power-law effective consistency coefficient in lbf-s$^{n'}$/ft^2, q_i is injection rate in bpm, h_f is fracture height in ft, X_f is the trial value of fracture length in ft.
The average fracture width can be calculated:

$$\bar{w} = \frac{\pi}{4} w_0 \quad (11)$$

where $\bar{w}$ is average fracture width in inch. The turbulent flow correction factor can be calculated as:

$$\beta = \frac{8 C_L \sqrt{\pi t}}{\pi \bar{w}} \quad (12)$$

where β is a turbulent flow correction factor (dimensionless), S_p is spurt loss in gal/100ft^2 typically from 0 to 50 gal/100ft^2 (Economides & Nolte, 2000), C_L is leak-off coefficient or fluid loss coefficient in ft/min$^{1/2}$ typically from 0.0005 to 0.05 ft/min$^{1/2}$ (Economides & Nolte, 2000), and t is injection time in second. The fracture length (X_f) can be calculated as:

$$x_f = \frac{[\bar{w}+2S_p]q_i}{64 h_f C_l^2}\left[\exp(\beta^2)\, erfc(\beta) + \frac{2\beta}{\sqrt{\pi}} - 1\right] \quad (13)$$

Later, the result of X_f calculation used for estimating the error percentage, as shown below:

$$\%error = X_{f\_input} - X_{f\_output} \quad (14)$$

Calculations of fracture width and length are stated to be correct if the %error obtained is between 0.00001 and -0.00001 (Yang, 2012). If the value of %error obtained greater than 0.00001 or lower than -0.00001, then the calculation must be repeated. Where the X_f inputted (in Eq.10) is the last calculation result of X_f (in Eq.13).
The dimensionless fracture conductivity is the ratio of the flow potential from the fracture to the well to that from the reservoir to the fracture (Yang, 2012). It can be calculated as shown:

$$C_{fD} = \frac{k_f \bar{w}}{k X_f} \quad (15)$$

where kf is fracture or proppant permeability in md, k is reservoir permeability in md, $\bar{w}$ is average fracture width in ft, and X_f is fracture length in ft.

RESULT AND DISCUSSION

Data needed are collected from a well of Meruap field, consist of well logging data, reservoir and rock properties, fracturing design (MFrac), and fracturing job data. These data are used to calculate the fracture geometry of hydraulic fracturing using the 2D model KGD (Khristianovic-Geertsma-de Klerk). This well actually had been performed hydraulic fracturing of KGD model in Air Benakat Formation based on assumptions explained by Geertsma & de Klerk (1969) and step-by-step explained by Economides and Nolte (2000).

The results obtained of fracture propagation solution are slurry and liquid volume injected, fluid loss volume, pumping time, net pressure, total fracture heigh, fracture half-length, max and average fracture width, fracture fluid efficiency. Afterward, results obtained of proppant design summary are propped fracture length, propped

fracture width, propped fracture height, fracture penetration ratio, fracture conductivity, dimensionless fracture conductivity, average fracture permeability, propped fracture ratio, closure time, and screen-out time.

The fracturing job was done in a target interval of 3720 – 3863 ftMD and defined as a pay zone. Data of rock mechanics obtained in the pay zone consist of Young's modulus with a range of 11.826 – 53.693 GPa and an average of 28.607 GPa. While Poisson's ratio is 0.196 – 0.321, with an average of 0.249. Figure 2 shows the most data of pay zone laying on the less brittle to brittle region. Grieser and Bray (2007) proposed that the brittle rocks exhibit a moderate to high Young's modulus and low Poisson's ratio, while the ductile rocks exhibit a low Young's modulus and high Poisson's ratio (Waliy et al., 2020a).

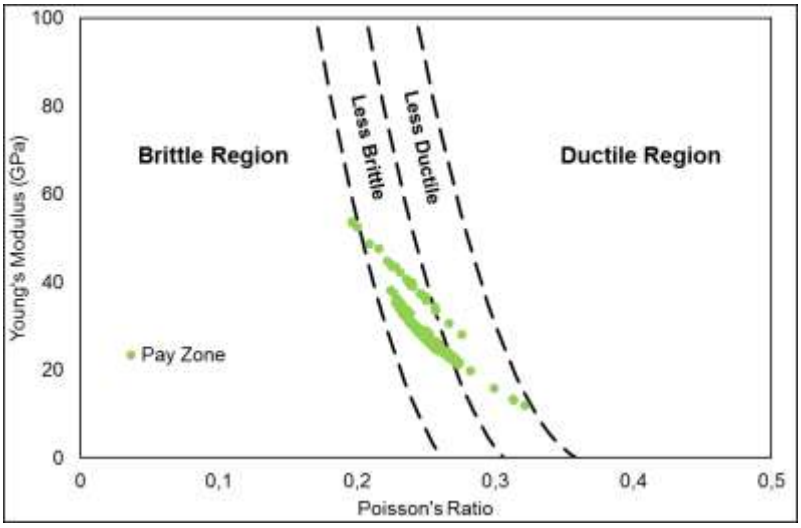

Figure 2. Cross plot of Young's modulus and Poisson's ratio

This paper is focused on the fracture length and width results to continue the analysis process. After 16 iterations of fracture geometry calculation, the results are obtained with a final error percentage of 7.4×10^{-10} %. This is valid according to the assumption used, the error percentage must be between 0.00001 and -0.00001. With the fracture height of 143 ft thick, the results of fracture geometry are respectively 57.552 ft and 0.231 inches of fracture length and average fracture width, while the dimensionless fracture conductivity is 4.449.

Rock mechanics are present explicitly in the equation explained by Economides and Nolte (2000) to calculate the fracture length and width. In step of estimating the plane strain modulus, Young's modulus and Poisson's ratio exist to represent the rock mechanics. This paper is intended to understand the effect of rock mechanics on fracture geometry and dimensionless fracture conductivity designed using KGD model. The way how to understand the effect of rock mechanics is by doing sensitivity analysis of Young's modulus and Poisson's ratio on fracture geometry and conductivity calculation. As the sensitivity of Poisson's ratio is analysing, the Young's modulus is being the

constant variable. It is likewise as the sensitivity of Young's modulus is analysing, the Poisson's ratio is being the constant variable (Waliy et al., 2020a).

Approximately 30 data of Young's modulus and Poisson's ratio respectively are used to do the sensitivity analysis. The sensitivity analysis of Young's modulus is carried out from calculations based on several iterations to obtain a valid result with an average of 16 iterations for each of 30 sensitivity data and have a final error percentage lower than -1.12×10^{-10} % and greater than 2.46×10^{-10} %. A cross plot of rock mechanics and fracture geometry (Fig. 3) is generated to understand the correlation between Young's modulus and fracture length/width.

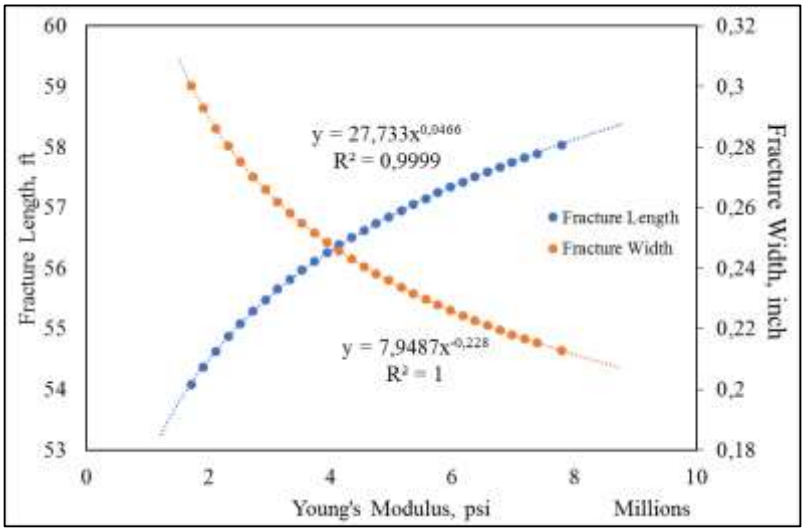

Figure 3. Cross plot of Young's modulus and fracture geometry

Based on Figure 3, there are empirical relationships between fracture length/width and Young's modulus, these are power regressions. The higher Young's modulus obtained, the fracture length goes longer, while the fracture width goes tiner. Otherwise, the lower Young's modulus obtained, the fracture length goes shorter, while the fracture width goes wider. These empirical relationships make easier to obtain fracture length and width from Young's modulus, as shown:

$$X_f = 27.733\ E^{-0.0466} \quad (15)$$

$$\bar{w} = 7.9487\ E^{-0.228} \quad (16)$$

where X_f is fracture length in ft, $\bar{w}$ is average fracture width in inch, and E is Young's modulus in psi. Both of these empirical relationships show coefficient correlations respectively of 0.9999 and 1. It means the empirical relationship between Young's modulus and fracture length/width is valid to apply in the study area.

The sensitivity analysis of Poisson's ratio is carried out from calculations based on several iterations to obtain a valid result with an average of 16 iterations for each of 30 sensitivity data and a final error percentage lower than -8.85×10^{-10} %. A cross plot of rock mechanics and fracture geometry (Fig. 4) is generated to understand the correlation between fracture length/width and Poisson's ratio.

International Journal of Petroleum and Gas Exploration Management
Vol.5, No.1, pp.1-14, March 2021
Published by ECRTD-UK
Print ISSN: (Print) ISSN 2515-0863
Online ISSN: (Online) ISSN 2515-0871

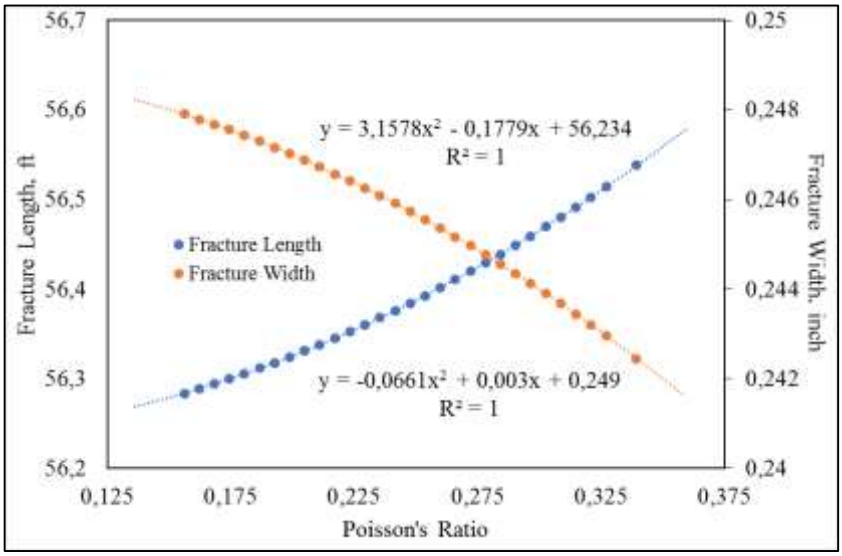

Figure 4. Cross plot of Poisson's ratio and fracture geometry

Based on Figure 4, there are empirical relationships between fracture length/width and Poisson's ratio, these are polynomial regressions. The higher Poisson's ratio obtained, the fracture length goes longer, while the fracture width goes tiner. Otherwise, the lower Poisson's ratio obtained, the fracture length goes shorter, while the fracture width goes wider. These empirical relationships make easier to obtain fracture length and width from Poisson's ratio, as shown below:

$$X_f = 3.1578\ v^2 - 0.1779\ v + 56.234 \quad (17)$$

$$\bar{w} = -0.0661\ v^2 + 0.003\ v + 0.\ 249 \quad (18)$$

where X_f is fracture length in ft, $\bar{w}$ is average fracture width in inch, and $\boldsymbol{v}$ is Poisson's ratio in fraction. Both of these empirical relationships show coefficient correlation of 1. It means the relationship between Poisson's ratio and fracture length/width is valid to apply in the study area.

The sensitivity analysis of dimensionless fracture conductivity is carried out based on sensitivity analysis of Young's modulus and Poisson's ratio on fracture length and width. It means 30 data were used to analyze the effect of Young's modulus and Poisson's ratio on dimensionless fracture conductivity. A cross plot (Fig. 5) is generated to understand the correlation between rock mechanics (Young's modulus and Poisson's ratio) and dimensionless fracture conductivity.

International Journal of Petroleum and Gas Exploration Management
Vol.5, No.1, pp.1-14, March 2021
Published by ECRTD-UK
Print ISSN: (Print) ISSN 2515-0863
Online ISSN: (Online) ISSN 2515-0871

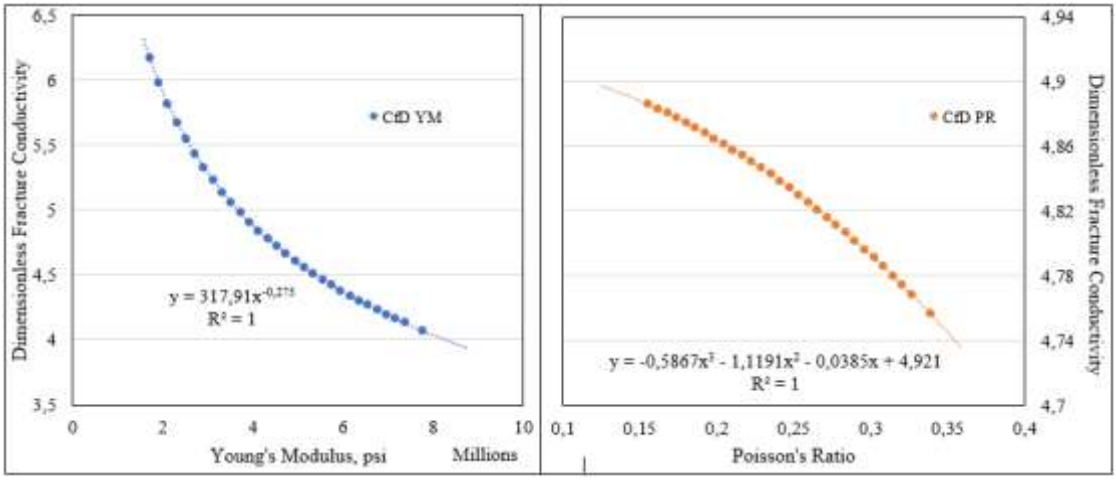

Figure 5. Cross plot of Young's modulus / Poisson's ratio and dimensionless fracture conductivity

Based on Figure 5, there are empirical relationships between Young's modulus or Poisson's ratio and dimensionless fracture conductivity, these are power and polynomial regressions. The higher Young's modulus or Poisson's ratio obtained, the dimensionless fracture conductivity goes lower. Otherwise, the lower Young's modulus or Poisson's ratio obtained, the dimensionless fracture conductivity goes higher. These empirical relationships make easier to obtain dimensionless fracture conductivity from Young's modulus or Poisson's ratio, as shown:

$$C_{fD\_E} = 317.91\ E^{-0.275} \quad (17)$$

$$C_{fD\_v} = -0.5867\ v^3 - 1.1191\ v^2 - 0.0385\ v + 4.921 \quad (18)$$

where C_{fD_E} is dimensionless fracture conductivity from Young's modulus, C_{fD_v} is dimensionless fracture conductivity from Poisson's ratio, E is Young's modulus in psi, and $\boldsymbol{v}$ is Poisson's ratio in fraction. Both of these empirical relationships show the coefficient correlation of 1. It means the relationship between Young's modulus / Poisson's ratio and dimensionless fracture conductivity is valid to apply in the study area.

CONCLUSION

The study has been carried out to understand the effect of rock mechanics on fracture geometry and dimensionless fracture conductivity of 2D model KGD based on sensitivity analysis. The focused study of rock mechanics are Young's modulus and Poisson's ratio, while the focused fracture geometry are fracture length and width. The actual fracturing job was done in a well of Meruap field. The results show that fracture geometry created are respectively 57.552 ft and 0.231 inches of fracture length and average fracture width, with a pay zone of 143 ft thick and dimensionless fracture conductivity of 4.449. The sensitivity analysis was focused on Young's modulus and Poisson's ratio.

The results present the same effect between Young's modulus and Poisson's ratio on the fracture geometry (fracture length and width) and dimensionless fracture conductivity. The higher Young's modulus or Poisson's ratio obtained, the fracture length goes longer, the fracture width goes tiner, while dimensionless fracture conductivity goes lower. Otherwise, the lower Young's modulus or Poisson's ratio obtained, the fracture length goes shorter, the fracture width goes wider, while dimensionless fracture conductivity goes higher. Integrated approaches of empirical relationship are also generated to estimate easily the dimensionless fracture conductivity and fracture geometry of fracture length and width with a certain value of Young's modulus and Poisson's ratio.

REFERENCES

Abe, H., Mura, T., & Keer, L. M. (1976). Growth Rate of a Penny-Shaped Crack in Hydraulic Fracturing of Rocks. *Journal of Geophysical Research, 81*(29), 5335-5340.

Biot, M., Masse, L., & Medlin, W. (1986). A Two-Dimensional Theory of Fracture Propagation. *SPE Annual Technical Conference and Exhibition* (pp. 17-30). New Orleans: SPE Production Engineering.

Buntoro, A., Prasetyadi, C., Wibowo, R. A., Suranto, & Lukmana, A. H. (2018). Validation of Shale Brittleness Index Calculation from Wireline Log of Well BETRO-001 by Using XRD Test Results and Uniaxial Test as Parameters for Determining Potential of Shale Hydrocarbon - Brown Shale of Pematang Group Formation. *ICEMINE, IOP Conference Series: Earth and Environmental Science, 212*(012069), 1-15.

Castagna, J. P., Batzle, M. L., & Eastwood, R. L. (1985). Relationships between Compressional-Wave and Shear-Wave Velocities in Elastic Silicate Rocks. *Geophysics, 50*(4), 571-581.

Castagna, J. P., Batzle, M. L., & Kan, T. K. (1993). Rock physics – The link between rock properties and AVO response, in J. P. Castagna and M. Backus, eds., Offset-dependent reflectivity – Theory and practice of AVO analysis. *Investigations in Geophysics, 8*, 135-171.

Chen, B., Barron, A. R., Owen, D. R., & Li, C.-F. (2018). Propagation of a Plane Strain Hydraulic Fracture With a Fluid Lag in Permeable Rock. *Journal of Applied Mechanics, 85*(091003), 1-10.

Dvorkin, J. (2007). Yet Another Vs Equation. *SEG Annual Meeting* (pp. 1570-1574). San Antonio: Society of Exploration Geophysicists.

Economides, M. J., & Nolte, K. G. (2000). *Reservoir Stimulation.* Wiley.

Fjær, E., Holt, R., Horsrud, P., Raaen, A. M., & Risnes, R. (2008). *Petroleum Related Rock Mechanics.* Kidlington: Elsevier Science Ltd.

Geertsma, J., & de Klerk, F. (1969). A Rapid Method of Predicting Width and Extent of Hydraulically Induced Fractures. *Journal of Petroleum Technology*, 1571-1581.

Geertsma, J., & Haafkens, R. (1979, March). A Comparison of the Theories for Predicting Width and Extent of Vertical Hydraulically Induced Fractures. *Journal of Energy Resources Technology, 101*, 8-19.

Gidley, J. L., Holditch, S. A., Nierode, D. E., & Veatch, R. W. (1989). *Recent Advances in Hydraulic Fracturing.* Society of Petroleum Engineers Inc.

Grieser, B., & Bray, J. (2007). Identification of Production Potential in Unconventional Reservoir. *SPE Production and Operations Symposium, 31 March-3 April, SPE 106623.* Oklahoma.

Heindl, R. A., & Mong, L. E. (1936). Young's Modulus of Elasticity, Strength, and Extensibility of Refractories in Tension. *Journal of Research of the National Bureau of Standards, 17*, 463-482.

Khristianovic, S. A., & Zheltov, Y. P. (1955). Formation of Vertical Fractures by Means of Highly Viscous Liquid. *4th World Petroleum Congress. WPC-6132*, pp. 579-586. Rome, Italy: World Petroleum Congress.

Kumar, J. (1976). The Effect of Poisson's Ratio on Rock Properties. *Society of Petroleum Engineers, SPE 6094*, 1-12.

Perkins, T. K., & Kern, L. R. (1961). Widths of Hydraulic Fractures. *SPE 36th Annual Fall Meeting. SPE 89*, pp. 937-949. Dallas, Texas: Journal of Petroleum Technology.

Waliy, F., Buntoro, A., Lukmana, A. H., & Rahma, A. A. (2020b). The Effect of Poisson's Ratio and Young's Modulus on Fracture Geometry of 2D Model PKN: Case Study of Unconventional Reservoir. *IATMI Simposium Professional Digital Presentation 2020.* Indonesia: Ikatan Ahli Teknik Perminyakan Indonesia.

Waliy, F., Prasetya, M. D., Rahma, A. A., Nugroho, W. A., & Herianto. (2020a). Shale Hydrocarbon Potential in Brown Shale of Pematang Formation Based on Total Organic Carbon Content and Geomechanic Approach. *International Journal of Petroleum and Gas Exploration Management, 4*(1), 21-32.

Yang, M. (2012). Hydraulic Fracture Production Optimization with a Pseudo-3D Model in Multi-Layered Lithology. *SPE International Symposium & Exhibition on Formation Damage. SPE 149833.* Lafayette, Louisiana: Society of Petroleum Engineers.

Yousefzadeh, A., Li, Q., Virues, C., & Aguilera, R. (2017). Comparison of PKN, KGD, Pseudo3D, and Diffusivity Models for Hydraulic Fracturing of the Horn River Basin Shale Gas Formations Using Microseismic Data. *SPE Unconventional Resources Conference, 15-16 February. SPE-185057-MS*, pp. 1-16. Calgary, Alberta: Society of Petroleum Engineers.

Zoback, M. D. (2007). *Reservoir Geomechanics.* Cambridge University Press.

International Journal of Petroleum and Gas Exploration Management
Vol.5, No.1, pp.1-14, March 2021
Published by ECRTD-UK
Print ISSN: (Print) ISSN 2515-0863
Online ISSN: (Online) ISSN 2515-0871

Appendix

Table 1.Young's modulus and Poisson's ratio data

Depth, ft	Young's Modulus	Poisson's Ratio	Depth, ft	Young's Modulus	Poisson's Ratio
3720	13.071	0.314	3795	26.576	0.252
3725	23.601	0.267	3800	28.432	0.246
3730	22.776	0.270	3805	27.953	0.247
3735	35.913	0.230	3810	27.435	0.250
3740	28.897	0.250	3815	30.377	0.240
3745	52.376	0.200	3820	29.056	0.244
3750	33.398	0.257	3825	26.120	0.253
3755	24.562	0.260	3830	27.864	0.247
3760	24.449	0.259	3835	29.198	0.244
3765	24.583	0.259	3840	25.033	0.257
3770	28.483	0.248	3845	27.322	0.249
3775	25.914	0.254	3850	25.966	0.253
3780	27.502	0.249	3855	25.004	0.257
3785	26.512	0.252	3860	34.879	0.230
3790	30.031	0.242	3863	33.358	0.234

Table 2.Fracturing design calculation of 2D model KGD

E', Pa	$X_{f(iteration)}$, m	$w_{(0)}$, m	$\bar{w}$, m	β	$X_{f(iteration+1)}$, m	%error
3.05E+10	43.586	0.02128621	0.01454337	2.90574872	14.016531	-29.5699
3.051E+10	14.01653	0.00684522	0.00467686	9.03583962	18.1990828	4.1826
3.051E+10	18.19908	0.00888785	0.00607244	6.95920380	17.2814764	-0.9176
3.051E+10	17.28148	0.00843972	0.00576627	7.32872139	17.4617672	0.1803
3.051E+10	17.46177	0.00852777	0.00582642	7.25305316	17.4255816	-0.0362
3.051E+10	17.42558	0.0085101	0.00581435	7.26811473	17.4328132	0.0072
3.051E+10	17.43281	0.00851363	0.00581676	7.26509971	17.4313667	-1.45E-03
3.051E+10	17.43137	0.00851292	0.00581628	7.26570257	17.431656	2.89E-04
3.051E+10	17.43166	0.00851306	0.00581638	7.26558200	17.4315981	-5.79E-05
3.051E+10	17.4316	0.00851303	0.00581636	7.26560611	17.4316097	1.16E-05
3.051E+10	17.43161	0.00851304	0.00581636	7.26560129	17.4316074	-2.31E-06
3.051E+10	17.43161	0.00851304	0.00581636	7.26560226	17.4316079	4.63E-07
3.051E+10	17.43161	0.00851304	0.00581636	7.26560206	17.4316078	-9.25E-08
3.051E+10	17.43161	0.00851304	0.00581636	7.26560210	17.4316078	1.85E-08
3.051E+10	17.43161	0.00851304	0.00581636	7.26560209	17.4316078	-3.70E-09
3.051E+10	17.43161	0.00851304	0.00581636	7.2656021	17.4316078	7.40E-10

International Journal of Petroleum and Gas Exploration Management
Vol.5, No.1, pp.1-14, March 2021
Published by ECRTD-UK
Print ISSN: (Print) ISSN 2515-0863
Online ISSN: (Online) ISSN 2515-0871

Table 3. Young's modulus sensitivity calculation of 2D model KGD

E, Gpa	v	X_f, ft	h_f, ft	$w_{(0)}$, in	$\bar{w}$, in	C_{fD}
11.8265	0.249427	54.07633	143	0.439557	0.3003186	6.1599598
13.2221	0.249427	54.3692	143	0.428601	0.2928327	5.9740576
14.6177	0.249427	54.63222	143	0.418964	0.2862487	5.8116247
16.0132	0.249427	54.87094	143	0.410384	0.2803869	5.667848
17.4088	0.249427	55.08947	143	0.402668	0.275115	5.5392184
18.8043	0.249427	55.291	143	0.39567	0.2703333	5.4231048
20.1999	0.249427	55.478	143	0.389276	0.2659649	5.3174873
21.5955	0.249427	55.65243	143	0.383398	0.2619492	5.2207847
22.9910	0.249427	55.8159	143	0.377966	0.2582376	5.1317372
24.3866	0.249427	55.96972	143	0.372921	0.2547908	5.0493264
25.7821	0.249427	56.11498	143	0.368216	0.2515763	4.9727184
27.1777	0.249427	56.25259	143	0.363812	0.2485673	4.9012219
28.5733	0.249427	56.38332	143	0.359676	0.245741	4.8342587
29.9688	0.249427	56.50785	143	0.355778	0.2430784	4.7713399
31.3644	0.249427	56.62674	143	0.352097	0.2405628	4.7120495
32.7600	0.249427	56.74049	143	0.34861	0.2381804	4.6560301
34.1555	0.249427	56.84954	143	0.345299	0.2359188	4.6029729
35.5511	0.249427	56.95426	143	0.34215	0.2337673	4.5526097
36.9466	0.249427	57.05499	143	0.339149	0.2317166	4.5047057
38.3422	0.249427	57.15203	143	0.336283	0.2297585	4.4590543
39.7378	0.249427	57.24565	143	0.333542	0.2278856	4.4154734
41.1333	0.249427	57.33608	143	0.330916	0.2260915	4.3738012
42.5289	0.249427	57.42354	143	0.328397	0.2243703	4.3338933
43.9244	0.249427	57.50823	143	0.325976	0.2227168	4.2956207
45.3200	0.249427	57.59031	143	0.323649	0.2211265	4.2588677
46.7156	0.249427	57.66995	143	0.321407	0.2195949	4.2235298
48.1111	0.249427	57.74729	143	0.319246	0.2181184	4.1895125
49.5067	0.249427	57.82246	143	0.31716	0.2166933	4.1567304
50.9023	0.249427	57.89559	143	0.315145	0.2153167	4.1251056
53.6934	0.249427	58.03614	143	0.311311	0.2126971	4.0650503

Table 4. Poisson's ratio sensitivity calculation of 2D model KGD

E, Gpa	v	X_f, ft	h_f, ft	$w_{(0)}$, in	$\bar{w}$, in	C_{fD}
28.60728	0.156082	56.28312	143	0.362842	0.2479045	4.885501
28.60728	0.162185	56.28832	143	0.362677	0.2477917	4.882827
28.60728	0.168288	56.29373	143	0.362505	0.2476744	4.880046
28.60728	0.174391	56.29936	143	0.362327	0.2475526	4.877158
28.60728	0.180494	56.3052	143	0.362142	0.2474262	4.874163
28.60728	0.186597	56.31125	143	0.36195	0.2472952	4.871059
28.60728	0.1927	56.31752	143	0.361752	0.2471597	4.867847
28.60728	0.198803	56.324	143	0.361547	0.2470195	4.864526
28.60728	0.204906	56.33071	143	0.361335	0.2468746	4.861094
28.60728	0.211009	56.33764	143	0.361116	0.2467251	4.857552
28.60728	0.217112	56.34479	143	0.36089	0.2465708	4.8539
28.60728	0.223215	56.35216	143	0.360657	0.2464118	4.850135
28.60728	0.229318	56.35976	143	0.360418	0.2462481	4.846258
28.60728	0.235421	56.36759	143	0.360171	0.2460795	4.842268
28.60728	0.241524	56.37565	143	0.359917	0.2459061	4.838164
28.60728	0.247627	56.38394	143	0.359656	0.2457278	4.833945
28.60728	0.25373	56.39246	143	0.359388	0.2455446	4.829611
28.60728	0.259833	56.40122	143	0.359113	0.2453565	4.825161
28.60728	0.265936	56.41023	143	0.35883	0.2451633	4.820594
28.60728	0.272039	56.41947	143	0.35854	0.2449652	4.815909
28.60728	0.278142	56.42895	143	0.358243	0.244762	4.811105
28.60728	0.284245	56.43869	143	0.357938	0.2445537	4.806182
28.60728	0.290348	56.44867	143	0.357625	0.2443402	4.801137
28.60728	0.296451	56.4589	143	0.357305	0.2441216	4.795972
28.60728	0.302554	56.46939	143	0.356978	0.2438977	4.790683
28.60728	0.308657	56.48013	143	0.356642	0.2436685	4.785271
28.60728	0.314759	56.49114	143	0.356299	0.243434	4.779734
28.60728	0.320862	56.50241	143	0.355948	0.2431941	4.774071
28.60728	0.326965	56.51395	143	0.355589	0.2429487	4.768281
28.60728	0.339171	56.53783	143	0.354846	0.2424415	4.756316